

## Sedimentation, Péclet number, and hydrodynamic screening

Kiley Benes,<sup>1</sup> Penger Tong,<sup>2</sup> and Bruce J. Ackerson<sup>1</sup>

<sup>1</sup>*Department of Physics, Oklahoma State University, Stillwater, Oklahoma 74078, USA*

<sup>2</sup>*Department of Physics, Hong Kong University of Science and Technology, Clear Water Bay, Kowloon, Hong Kong*

(Received 13 January 2007; revised manuscript received 7 May 2007; published 8 November 2007)

The sedimentation of hard spheres in a Newtonian solvent is studied as a function of Péclet number in the low-concentration limit. Two functional forms for the sedimentation velocity as a function of particle concentration are realized in the limit of high and low Péclet numbers. We argue that a more ordered phase occurs for large Péclet numbers. Measurements of settling in sheared suspensions support these contentions. Recent explanations of sedimentation in suspensions are examined in light of these results.

DOI: [10.1103/PhysRevE.76.056302](https://doi.org/10.1103/PhysRevE.76.056302)

PACS number(s): 47.57.-s, 83.80.Hj, 05.40.-a, 83.10.Pp

### I. INTRODUCTION

The sedimentation of a collection of uniformly sized spheres in a Newtonian solvent represents one of the simplest nonequilibrium processes. Sedimentation has long been recognized as a medical diagnostic tool [1] and as an analytic tool to determine macromolecular dimensions [2]. These techniques typically determine macromolecular dimensions using the Stokes velocity  $U_0 = 2\Delta\rho g a^2 / (9\eta)$  for sedimentation measurements in the limit of infinite dilution. Here  $a$  is the sphere radius,  $\eta$  is the solvent viscosity,  $g$  is the acceleration of gravity, and  $\Delta\rho$  is the particle-solvent density difference. Batchelor [3] determined the first-order concentration correction to the Stokes velocity. He assumed (i) a low particle Reynolds number (or the neglect of inertia), (ii) two-body hydrodynamic interactions, (iii) a random particle distribution in space, and (iv) the system size infinite in the direction transverse to the settling. The result is given in terms of the particle pair correlation function  $g(r)$  and the particle volume fraction  $\phi$ :

$$U = U_0[1 - (5 + \alpha)\phi],$$

$$\alpha = 3 \int_2^\infty x[1 - g(x)]dx + \frac{15}{4} \int_2^\infty \frac{g(x)}{x^2} dx, \quad (1)$$

where  $x = r/a$  with  $r$  being the interparticle separation. For a dilute hard-sphere interaction, the integrations are readily performed to find

$$U = U_0(1 - 6.55\phi + \dots). \quad (2)$$

Direct particle interactions influence the form of the pair distribution function  $g(r)$ . A repulsive interaction between particles decreases the sedimentation velocity  $U$ , while an attractive interaction increases the sedimentation velocity compared to the hard-sphere result given in Eq. (2). Mazur and van Saarloos [4] generalized the Batchelor result to larger particle concentrations. Experimentally the concentration dependence of the sedimentation velocity for hard spheres is known [5,6].

Recent measurements [7] of sedimentation in dilute suspensions of charged spheres produced a different functional form from that given in Eq. (2). The experimental results produce the following “nonanalytic” form:

$$U = U_0(1 - k\phi^{1/3} + \dots), \quad (3)$$

where  $k \approx 2.8$ . Thies-Weesie *et al.* explain the above nonanalytic form using the rescaled mean spherical approximation (RMSA) pair distribution function for a screened Coulomb interaction between the charged particles. While they utilize the relationship between diffusion and sedimentation to predict sedimentation velocities, the same results can also be obtained using the Batchelor formalism. Intuitively, the repulsive charge interaction between spheres is so strong that the spheres maintain as large a separation from one another as possible. Under these conditions, the position of the primary maximum in the pair distribution function scales as the mean particle separation,  $\ell \sim a\phi^{-1/3}$ . This unanticipated concentration dependence in the pair distribution function modifies the concentration dependence given in Eq. (2) to produce the form in Eq. (3).

While Batchelor produced the result given in Eq. (2) for a dilute random mixture of hard spheres, the prediction for a random array of *fixed* spheres gives [8–11]

$$U = U_0(1 - \tilde{k}\phi^{1/2} + \dots), \quad (4)$$

and for a *fixed* array of ordered spheres the result is identical to Eq. (3) with the value of  $k$  depending on the crystal structure [10,12–14]. Thies-Weesie *et al.* [7] provided intuition for these results: the change in concentration dependence going from Eq. (2) to Eq. (4) and to Eq. (3) “is due to the successive switching off of Brownian motion and the positioning of spheres on an ordered array. Each step deprives particles of possibilities to ‘screen’ each other from the back-flow and hence increases the friction per particle.”

Some time ago, Oliver [15] compiled data for the sedimentation velocity measured for dilute suspensions of spheres larger than those quoted above. Remarkably these suspensions produced the same concentration dependence as that given in Eq. (3). Oliver rationalized this concentration dependence by arguing that the interparticle separation is governed, not by the particle diameter, but again by the relationship  $\ell \sim a\phi^{-1/3}$ . The particles find themselves as far away from one another as possible. But Oliver gives no mechanism producing this order. Presumably these large particles are hard spheres with little direct interaction, as compared to the charged spheres discussed above. Surely these

dilute suspensions are not crystalline arrays but are “random” distributions of freely moving hard spheres.

Systems composed of larger or more dense hard spheres exhibit a variety of strange or seemingly contradictory behavior. Tory *et al.* [16] presented a variety of observations for monodisperse particle suspensions that demonstrate this remarkable complexity of behavior. The suspension-supernatant interface becomes diffuse in dilute suspensions and falls with a rate that is remarkably constant and less than the Stokes velocity  $U_0$  [15,17–19]. The interior of the suspension shows large particle velocity variation up to 4 times faster than the mean settling velocity [15,17,20–23]. Large clusters of spheres settle more rapidly with fluid flowing around rather than through them [20–22]. The variance of particle velocities increases rapidly with volume fraction in the range from  $10^{-3}$  to  $10^{-2}$  [20–22,24] and as the container to particle size ratio increases [17]. Similarly, the mean internal settling velocity increases with volume fraction and the container to particle size ratio. The mean internal velocity is greater than the Stokes velocity and hence is also greater than the suspension interface velocity [17,20,21,24]. The volume fraction of the particles evidences a gradient at the suspension-supernatant interface. This gradient grows with time so that the interface becomes less distinct [19].

In addition to the study of mean settling velocities, velocity fluctuations received renewed and intense attention after Calffisch and Luke [25] showed theoretically using the Batchelor assumptions that the velocity fluctuations depend on the linear dimension of the container and grow without limit as the sample container grows to infinite size. The velocity fluctuations have been studied experimentally [26–32] and theoretically [20,33–35] and by computer simulation [36–40]. Experiments have not yet resolved whether the velocity fluctuations can reach a steady state independent of container size [27,29] or continue to evolve [31,41]. Theoretically, it is recognized that horizontal boundaries at the top and bottom of a suspension and the presence of the suspension-supernatant boundary strongly influence the time evolution of velocity fluctuations. From computer simulations Nguyen and Ladd [42] argue that the suspension becomes more uniform as large-scale particle density fluctuations rise or sink out of the suspension. As the density fluctuations drain out, the velocity fluctuations decrease in magnitude. Alternatively, Mucha *et al.* [43] argue that velocity fluctuations decrease in magnitude as the suspension becomes stratified. The stratification, however slight, stabilizes the movement of density fluctuations and suppresses velocity fluctuations.

In the experiment presented here, we measure the mean sedimentation velocity of monodisperse suspensions of hard spheres as a function of the Péclet number, which characterizes the strength of convection to that of diffusion. When the Péclet number is small, Brownian motion is significant and the particle configurations are continuously randomized, such that the Batchelor result is expected to hold. When the Péclet number is large, convection dominates, and for reasons described above the suspension becomes more uniform or stratified as compared to a random system. This should be evident in the mean settling velocity as well as in velocity fluctuations. Care is taken to eliminate any direct interaction

TABLE I. Particle samples used in the present experiment and in literature data.

Sample	$a$ ( $\mu\text{m}$ )	Pe	Manufacturer and reference
PS1	$20.94 \pm 0.42$	$9.8 \times 10^4$	Bangs Laboratories
PS2	$10.15 \pm 0.2$	$5.4 \times 10^3$	Bangs Laboratories
PS3	$7.45 \pm 0.15$	$1.6 \times 10^3$	Bangs Laboratories
PS4	$2.55 \pm 0.05$	$2.1 \times 10^1$	Bangs Laboratories
PS5	$1.05 \pm 0.02$	$6.8 \times 10^{-1}$	Bangs Laboratories
CP1	$0.38 \pm 0.01$	$4.8 \times 10^{-2}$	Ref. [50]
PMMA	$80.5 \times 10^3$	$8.5 \times 10^7$	Ref. [15]

between particles to avoid the effect of the screened Coulomb potential for charged particles, as measured by Thies-Weesie *et al.* [7]. To further verify the thesis that particle ordering produces the nonanalytic concentration dependence, new sedimentation measurements are made for suspensions undergoing a simple shear flow, which is applied to destroy local and global interparticle structures.

## II. EXPERIMENT

### A. Measurement of the mean settling velocity

Five polystyrene particle samples of different sizes are used in the experiment. They were purchased from Bangs Laboratories Inc. (Dynaspheres) and are suspended in water. In Table I we give the values of the radius  $a$  and the Péclet number Pe of each particle sample. The values of  $a$  are provided by the manufacturer. The polydispersity (ratio of the standard deviation to the mean size) of each sample is 2% or less. The Péclet number is given by  $\text{Pe} = aU_0/D_0 = (4\pi/3)\Delta\rho g a^4 / (k_B T)$ , where  $D_0 = k_B T / (6\pi\eta a)$  is the Stokes-Einstein diffusion constant for individual particles. The Péclet number measures the importance of convection compared to diffusion. Because the particles as received are charge stabilized against aggregation by added surfactant, aliquots of different volume fraction particles are prepared using Barnsted de-ionized water (10 M $\Omega$ ) with added sodium chloride (NaCl) to screen the interparticle charge interactions and sodium dodecylsulphate (SDS, 0.05% by weight) to maintain charge stabilization, albeit at very small screening lengths.

The suspension settling velocity was measured, and a known amount of salt was added. The settling velocity was remeasured, correcting for changes in the solvent density. The process was repeated until the measured settling rates saturated. For salt concentrations 0.1 M and greater, the measured sedimentation velocities for a given particle size saturated to the values reported here. We conclude that under this condition the ionic screening is sufficiently great that the only direct interaction between the particles is well represented by the hard-sphere interaction potential.

The samples fill 1.5-ml or 5-ml screw-top vials, where the sample heights are 3.5 cm or 4.5 cm, respectively. Even with these small volumes the ratio of the smallest cell dimension to the particle radius is greater than 350. The effect of con-

tainer boundaries on the settling velocity of a sphere at the center of a spherical volume, having a radius 350 times the sphere radius, is less than 1% different from the velocity for an infinite volume [18]. In Bruneau *et al.* [44], Eq. (A5) provides a correction for wall effects by integrating over the container dimension. The magnitude of this correction is less than 2% for the largest particles we used and much less than that for the rest.

The samples are mixed in the sealed vials by slow tumbling end over end using a mechanical mixer. They are also tumbled by hand prior to measurement. After mixing, these vials are placed in a well stirred water bath to control temperature to  $20 \pm 0.1$  °C, but more importantly to eliminate temperature gradients [45]. Each particle size series has samples with volume fraction  $\phi$  in the range from  $5 \times 10^{-5}$  to  $5 \times 10^{-2}$ . The sedimentation velocity of each sample is determined by measuring the settling speed of the particle-supernatant interface, which is measured to within  $10 \mu\text{m}$  using a cathetometer. Typically five measurements are taken per sample over a period up to a few hours. All height versus time measurements show linear dependence ( $R^2 > 0.99$ ) with typical precision of  $\sim 5\%$  for the fitted slope from the repeated measurements.

We determine the density of polystyrene particles by measuring the sedimentation velocity of dilute samples in known mixtures of  $\text{D}_2\text{O}$  and  $\text{H}_2\text{O}$ , the former having a density greater than the particles and the latter a density less than the particles. For a mixture of solvents corresponding to density match with the particles, the sedimentation velocity is zero. From the sedimentation measurements in mixtures of different  $\text{D}_2\text{O}$  mass fraction, we find that the density match occurs at the  $\text{D}_2\text{O}$  mass fraction of 0.5066 and corresponds to a particle density  $\rho_p = 1.052 \text{ g/cm}^3$ , assuming volume conservation on mixing the two forms of water. This value of  $\rho_p$  agrees well with the literature value for polystyrene latex spheres. Pycnometer measurements give the densities of various salt, soap, and water mixtures used in the experiment. These values are used in the calculation of the Péclet numbers shown in Table I.

### B. Measurement of the mean settling velocity under a shear

Polystyrene particles having a radius  $a = 10.15 \mu\text{m}$  (PS2 in Table I) are suspended at the volume fraction  $\phi = 5 \times 10^{-3}$  in water with added NaCl and SDS as described above. The suspension is contained in a Couette shear cell [46]. The shear cell is composed of two concentric cylinders. The outer radius of the inner cylinder is  $R_1 = 1.45 \text{ cm}$ , and the gap between the cylinders is  $h = 0.58 \text{ cm}$ . The height of the sample is  $4.5 \text{ cm}$ . The inner cylinder is powered by a stepping motor having 200 steps per revolution with the pulse rate under software control. The rotation is smooth for large angular frequencies, but is a pulsed motion at low rates of rotation. Therefore, data at selected low rotation rates are reproduced with a continuously driven dc motor. The shear rate varies across the gap, and we give the rate at the inner cylinder wall. Because the inner wall is moving, the suspension is subject to the Taylor-Couette instability [47]. The critical rotation rate for the onset of the instability is  $\Omega_c$

$= 41.3 \nu / (h^{3/2} R_2^{1/2})$ , where  $h = R_2 - R_1$  and  $\nu$  is the kinematic viscosity of the fluid. For our cell with inner radius  $R_1 = 1.45 \text{ cm}$  and outer radius  $R_2 = 2.03 \text{ cm}$ , we have  $\Omega_c = 0.67 \text{ rad/s}$ . We do in fact observe the onset of this instability at the predicted value of  $\Omega_c$ . The interface between the settling suspension and clear supernatant above tips either towards the inner or outer cylinder as it passes through different portions of the convective rolls. But for sufficiently small rotation rates, the interface remains flat, albeit a sensitive indicator of convective motion.

The inner cylinder rests on a liquid mercury seal to exclude the suspension from the region beneath the inner cylinder. The mercury seal allows free rotation of the inner cylinder. Without the mercury seal, the suspension becomes unstable while settling. As the particles settle away from the bottom of the inner cylinder, a solvent bubble develops in contact with the cylinder end. The bubble eventually creeps up the vertical cylinder walls and makes the suspension unstable. The whole shear cell is immersed in a well stirred water bath to eliminate convection due to temperature gradients. The temperature is controlled to within  $0.1$  °C for the duration of the measurements. Samples in the shear cell are mixed by raising the inner cylinder out from the sample and lowering back into the sample several times prior to measurement. Convection and turbulence mix the sample. The suspension height is monitored as a function of time to within  $10 \mu\text{m}$  using a cathetometer.

The interface between the sedimenting suspension and supernatant becomes more diffuse with increasing hydrodynamic diffusion and polydispersity. The interface also becomes more diffuse in time with hydrodynamic diffusion being more dominant at early times [19]. The reduced hydrodynamic diffusion constant  $\hat{D} = D_h / (U_0 a)$  depends on the volume fraction and has a value typically greater than unity and less than 15. For volume fractions less than 0.01 it is essentially unity [19]. As a result the diffusion constant in the dimensionless diffusion equation becomes  $\hat{D} a / H_0$  or  $a / H_0$  at small volume fractions. The interface spreading increases with increasing particle radius at fixed sample height  $H_0$ .

In determining the settling velocity of the samples, we made direct visual observations of the interface rather than light transmission measurements [19,48]. However, we restricted our measurements to the initial settling process in the upper quarter of the sample containers. Observation times were adjusted to account for the different settling rates. In this region the interface is the least diffuse and our measurements produce linear plots of interface height versus time to a high degree of precision. Numerically integrating the dimensionless drift-diffusion equation, using unity for the reduced hydrodynamic diffusion constant, indicates insignificant interface spreading (less than a few percent of the height) for all but the largest Pe value sample measured.

## III. EXPERIMENTAL RESULTS

Figure 1 presents the measured sedimentation velocity  $U$  normalized by the Stokes velocity  $U_0$ . The solvent density is corrected for the amount of added salt using standard tables

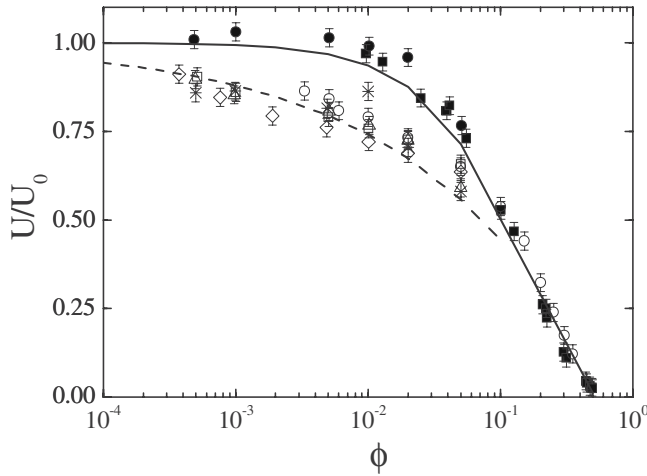


FIG. 1. Normalized sedimentation velocity  $U/U_0$  as a function of volume fraction  $\phi$  for hard spheres with the Péclet number  $Pe = 4.8 \times 10^{-2}$  (solid squares),  $6.8 \times 10^{-1}$  (solid circles),  $2.1 \times 10^1$  (stars),  $1.6 \times 10^3$  (open triangles),  $5.4 \times 10^3$  (open diamonds),  $9.8 \times 10^4$  (open squares), and  $8.5 \times 10^7$  (open circles). The solid line shows the function  $U/U_0 = (1 - \phi)^{6.55}$ , and the dashed line shows the function  $U/U_0 = 1 - 1.2\phi^{1/3}$ .

[49]. In addition, literature data are included for the lowest [50] and highest [15] Péclet numbers. The lowest  $Pe$  system ( $Pe = 4.8 \times 10^{-2}$ ) is a suspension of  $0.38\text{-}\mu\text{m}$ -radius hard spheres made of a copolymer core of methylmethacrylate and trifluoroethylacrylate stabilized by a poly-12-hydroxystearic acid coating and suspended in *cis*-decaline. The largest  $Pe$  sample ( $Pe = 8.5 \times 10^7$ ) is comprised of Kallodoc (polymethylmethacrylate) spheres with a mean radius  $a = 80.5\text{ nm}$  in mixtures of glycerol and water. The large  $Pe$  particles settle more slowly compared to the smaller  $Pe$  particles. In the data presented here, the salt concentration is order  $0.1\text{ M}$ , giving a Debye screening length less than  $10\text{ nm}$ . The polystyrene particles, though charged to prevent coagulation, are highly screened and should behave effectively as hard spheres. Evidently the data shown in Fig. 1 separate into two different curves. For data with  $Pe < 1$ , the approximation  $U/U_0 = (1 - \phi)^{6.55}$  (solid line) represents the data well and reduces to the Batchelor prediction  $U/U_0 \approx 1 - 6.55\phi$  at small volume fractions. [We notice that the approximation  $U/U_0 = (1 - \phi)^{5.55}$  fits the high- $\phi$  portion of the data slightly better and was also used in the literature [51].] On the other hand, for  $Pe > 1$  the form  $U/U_0 = 1 - 1.2\phi^{1/3}$  gives a better fit to the data at small values of  $\phi$ .

To test the possibility that ordering influences the settling rate for large  $Pe$  suspensions, we perform sedimentation measurements on selected suspensions subjected to a shear flow. A shear directed perpendicular to the direction of settling will advect the particles along streamlines perpendicular to the direction of settling, moving some particles closer together (along the direction of compression) and pulling other particles further apart (along the direction of extension). In general, a horizontal shear flow should only influence the interparticle ordering, but not mix the suspension vertically; any stratification in the suspension should remain.

Figure 2 shows the measured sedimentation velocity  $U/U_0$  as a function of cylinder rotation rate (or shear rate)  $\Omega$

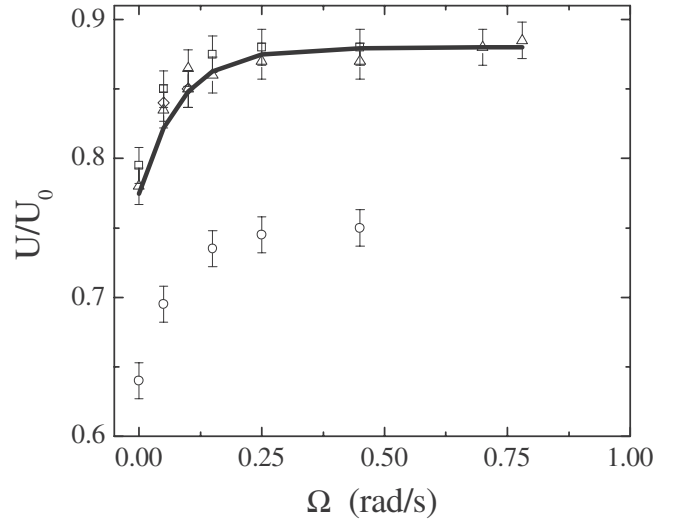


FIG. 2. Normalized sedimentation velocity  $U/U_0$  as a function of cylinder rotation rate  $\Omega$ . The measurements are made at three salt (NaCl) concentrations:  $0\text{ M}$  (unscreened particles, circles),  $0.06\text{ M}$  (squares), and  $0.12\text{ M}$  (triangles). The diamonds are obtained using the continuous dc motor. The solid curve shows the fitted function  $U/U_0 = \alpha[1 - \beta \exp(-\tau\Omega)]$  with  $\alpha = 0.88$ ,  $\beta = 0.12$ , and  $\tau = 12\text{ s}$ .

at fixed  $\phi = 5 \times 10^{-3}$ . It is seen that the measured  $U/U_0$  for the PS2 particles increases with increasing shear rate  $\Omega$ . The lower curve for the unscreened particle suspension indicates that there are significant direct repulsions between the particles. However, adding NaCl to obtain a  $0.06\text{-M}$  concentration produces results which have saturated and change no further when the salt concentration is increased to  $0.12\text{ M}$ . With Debye screening length less than  $10\text{ nm}$ , the particles are well screened and act as hard spheres. The measured  $U/U_0$  increases from the stationary suspension value (at  $\Omega = 0$ ) to nearly the value predicted by Batchelor for low- $Pe$  suspensions. This transition is consistent with the hypothesis that the particle ordering during the sedimentation in high- $Pe$  suspensions is not random. Presumably the shear flow produces a more random structure to obtain nearly the Batchelor result. This is achieved when the shear rate  $\Omega$  becomes larger than the relaxation rate  $1/\tau$  of the system to the nonrandom quiescent suspension structure. The value of the relaxation time  $\tau$  is determined by fitting the data in Fig. 2 to the exponential form,  $U/U_0 = \alpha[1 - \beta \exp(-\tau\Omega)]$ , giving  $\tau = 12\text{ s}$  (solid curve). This time is comparable to that taken for a suspended particle to settle on the order of an interparticle spacing  $\ell$ , a sufficient distance to induce some degree of collective ordering in the absence of diffusion.

#### IV. DISCUSSION

The literature includes measurements of suspension settling velocity for a range of  $Pe$  values. For large  $Pe$ , both linear [Eq. (2)] [44,52,53] and nonanalytic [Eq. (3)] [7,15] results are reported. Oliver [15] cites the work of Hanratty and Bandukwala [52], which shows a linear volume fraction dependence as compared to a wealth of other data, cited by Oliver, demonstrating a nonanalytic volume fraction depen-

dence. No quantitative estimate of polydispersity is available for the Hanratty-Bandukwala data, but the data showing the nonanalytic volume fraction dependence evidence low polydispersity on the order of 5%. Bruneau *et al.* [44] perform x-ray transmission measurements of settling of polydisperse suspensions and mixtures. The minimum volume fraction is 0.1%, and the data are characterized by a linear function in volume fraction with a coefficient 5.3. This is near the expected value for polydisperse suspensions [51]. However, the samples have large polydispersity. Similarly, Ham and Homsy [53] make tracer diffusion-settling measurements within settling suspensions with volume fractions greater than 2.5%. They observe large velocity fluctuations and characterize data by a linear volume fraction theory with a coefficient 4. Like Bruneau *et al.*, the samples had a large polydispersity with particle sizes varied on the order of 20% of the mean value. We conclude that large polydispersity may hinder subtle structure formation due to the increased internal chaos produced by particle size separation and produce a linear volume fraction dependence for the settling velocity.

The introduction presents two functional forms for the normalized sedimentation velocity  $U/U_0$  at low volume fractions. The Batchelor form given in Eq. (2) is realized for Péclet number less than unity, small Reynolds number, and hard-sphere interactions. The Brownian motion of the particles keeps particles randomly positioned. On the other hand, the “nonanalytic” form given in Eq. (3) obtains for Péclet number greater than unity or for Péclet number less than unity, if the particle direct interaction is strong and long ranged such as that given by an appropriate screened Coulomb interaction [7,54]. Here the particles are held as far from one another as possible without forming a crystal structure. The results for the strongly interacting system suggest that during the sedimentation the large Pe suspensions are similarly ordered. Indeed, Oliver [15] suggested such ordering some 40 years earlier. However, the nature and mechanism of ordering are unclear.

Recent work showed that velocity fluctuations in sedimentation are also related to subtle particle ordering [30,40,42]. Poisson or purely random fluctuations produce the largest velocity fluctuations initially. As the velocity fluctuations decrease, the particle occupation statistics deviate from Poisson and the structure factor  $S(q)$  at vanishing wave number  $q$  tends to zero. The suspension becomes more ordered, more uniform, on large length scales. Evidently, the large-scale random fluctuations away from the average particle concentration fall or rise out of the system.

Mucha *et al.* rationalize the experimental, theoretical, and computer simulation results for velocity fluctuations in a recent publication [43]. Non-Poisson occupation statistics play an essential role. They also postulate a weak concentration gradient to stabilize concentration fluctuations and suppress velocity fluctuations [33]. A simple model based on a continuum hydrodynamic model [43] produces a static structure factor  $S(q)$  for the settling suspension:

$$S(q) = \frac{Nq^2}{Dq^2 + A\beta U\phi[(aq)^2 + (ad)^2]}, \quad (5)$$

where  $N$  is the noise strength,  $D$  is the diffusivity,  $A$  is an arbitrary constant,  $\beta$  is the vertical concentration gradient,  $U$

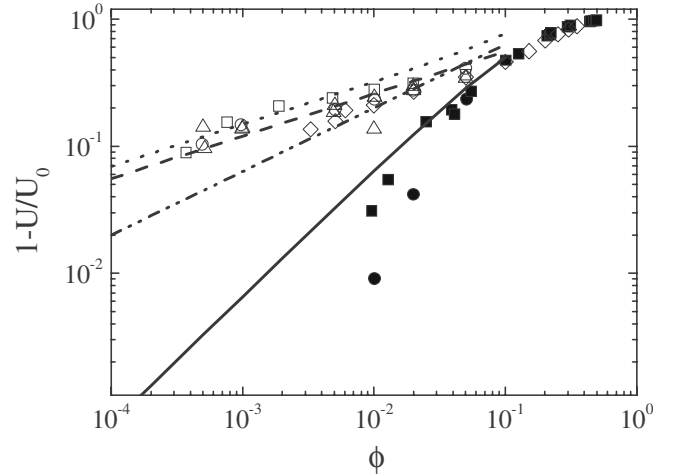


FIG. 3. Log-log plot of  $1-U/U_0$  versus the volume fraction  $\phi$ . The velocity data  $U/U_0$  used here are the same as those shown in Fig. 1. The solid line represents  $1-U/U_0=1-(1-\phi)^{6.55}$ , while the dashed line represents  $1-U/U_0=1.2\phi^{1/3}$ . The dotted line shows Eq. (8) with  $\xi(t)=1$ , and the dot-dashed line shows Eq. (4) with  $\tilde{k}=2$  (see text). The estimated 5% experimental error produces large scatter as  $1-U/U_0$  approaches zero.

is the average settling velocity,  $\phi$  is the initial volume fraction, and  $a$  is the particle radius. Stratification introduces another length scale  $d$ , the minimum cell dimension. This structure factor evidences reduced particle number fluctuations. The pair correlation function  $g(r)$  represented by this structure factor for  $D=N$  has the screened Coulomb form

$$g(r) = 1 + \frac{2\pi^2 B(e^{-\gamma r} - e^{-\sqrt{Br}\gamma})}{\gamma^2 r}, \quad (6)$$

where  $B=A\beta U\phi a^2/D$  and  $\gamma=a/d$ . The screened Coulomb form in Eq. (6) produces a normalized settling velocity  $U/U_0$  like that given in Eq. (4) [54], but not the experimentally observed form in Eq. (3). A comparison of the two forms with data is shown in Fig. 3. In addition, the assumption of an extremely weak (possibly not measurable) particle concentration gradient may not be justified [55].

Another model represents the order in the suspension as a hard-sphere pair correlation function. However, the effective hard-sphere radius grows with time from the particle size  $2a$  to a value equal to the interparticle separation,  $\ell \sim a\phi^{-1/3}$ , due to self-cleaning of fluctuations in density. The pair correlation function is taken as

$$g(r) = H(r - \xi(t)a\phi^{-1/3}), \quad (7)$$

where  $H(r - \xi(t)a\phi^{-1/3})$  is the Heaviside step function and  $2\phi^{1/3} \leq \xi(t) \leq 1$ . With this pair correlation function both the number fluctuations and the average settling velocity are calculated. Using Eq. (1) we find

$$U = U_0 \left( 1 - \frac{3}{2} \xi^2(t) \phi^{1/3} + \phi - \frac{15}{4\xi(t)} \phi^{4/3} \right). \quad (8)$$

This equation has the desired volume fraction dependence with a coefficient  $3\xi^2(t)/2$  and is presented in Fig. 3 with

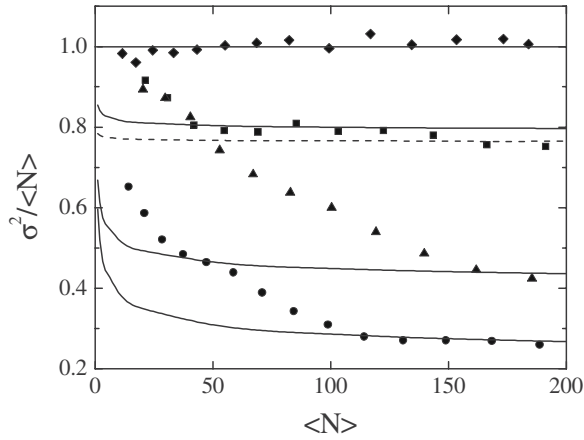


FIG. 4. Reduced number fluctuations  $\sigma^2/\langle N \rangle$  as a function of the average number of particles in the test volume,  $\langle N \rangle$ . The measurements were made at different times during the sedimentation: 2 min (diamonds), 4 h (squares), 6 h (triangles), and 8 h (circles). The solid lines are calculated using Eq. (10) with  $\xi(t)=0, 0.6, 0.85$ , and  $0.93$  from top to bottom, respectively. The dashed line comes from the work of Nguyen and Ladd (see text).

$\xi(t)=1$  (dotted line). It is seen that the dotted line overestimates the measured  $1-U/U_0$  slightly. The growth factor  $\xi(t)$ , of course, depends on the details of the pair correlation function  $g(r)$ . By choosing  $\xi(t)=0.9$ , we find that Eq. (8) fits the data as well as Eq. (3) does (not shown).

We have not been able to model the work by Nguyen and Ladd [42] to produce a normalized sedimentation velocity  $U/U_0$ . Felderhof [35] recently published a paper for velocity fluctuations. This work does not assume a vertically bounded system and so is quite different from the work presented here. However, the theory does predict the form in Eq. (3), but the coefficient  $k=0.006$  is very small and assumed unobservable.

For the occupation statistics, we use the form given by Lei *et al.* [30]:

$$\frac{\sigma^2}{\langle N \rangle} = 1 + \frac{\phi}{\nu_p} \int F(\mathbf{r})(g(r) - 1) d\mathbf{r}, \quad (9)$$

where  $\sigma^2/\langle N \rangle = \langle N^2 - \langle N \rangle^2 \rangle / \langle N \rangle$  is the number fluctuations normalized by the mean number of particle  $\langle N \rangle$  in the observation volume  $V$ ,  $\nu_p = (4\pi/3)a^3$  is the particle volume, and  $F(\mathbf{r})$  is a convolution of the observation volume with itself. We take the observation volume to be simpler than that in the experiment, a sphere of radius  $R$ . Then Eq. (9) produces

$$\frac{\sigma^2}{\langle N \rangle} = 1 - \xi^3(t) \left( 1 - \frac{9\xi(t)}{16\langle N \rangle^{1/3}} + \frac{\xi^3(t)}{32\langle N \rangle} \right). \quad (10)$$

Figure 4 compares occupation statistics data of the PS1 particles obtained by Lei *et al.* [30] with the form given in Eq. (10). Samples are mixed the same way in the mean settling velocity experiments and in the occupation statistics experiment. The reader should refer to the paper by Lei *et al.* [30] for further details. Here  $\xi(t)$  is adjusted between  $2\phi^{1/3}$  and 1 to fit the data. While there is a qualitative agreement, the measured  $\sigma^2/\langle N \rangle$  decays more slowly with  $\langle N \rangle$  than the

theory predicts. This is possibly due to the observation volume being more pancake shaped than spherical in the experiment. The theory of Mucha *et al.* [43] fits the number fluctuation data better, though it fails to produce the correct functional form for the settling velocity. The dashed line represents the number fluctuations predicted by the structure factor of Levine *et al.* [56] using numerical values from the simulations of Nguyen and Ladd [42]. This structure factor is related to  $g(r)$  in Eq. (9) to obtain the results shown in Fig. 4.

Figure 4 shows that particle ordering and suppression of density fluctuations in the lower third of the suspension occur on time scales far longer (by a few orders of magnitude) than the relaxation time for the interface shown in Fig. 2. To understand how this time-scale difference may come about, consider the typical container size concentration fluctuation due to random positioning of the particles. For the most dilute sample (PS1 particles with  $\phi=5 \times 10^{-4}$ ), there are roughly  $N=10^4$  particles in a cubic centimeter. Our samples are typically more than  $1 \text{ cm}^3$  but  $10^4$  is a convenient number. For random fluctuations in particle placement (Poisson statistics), sample size particle concentration variations are on the order of  $\sqrt{N}$  or a  $\sqrt{N}/N=1\%$  variation in particle concentration throughout the volume. It is not much, but this is what must be smoothed out or settle out to make the sample more uniform and quench velocity fluctuations. In terms of concentration change, it is probably not measurable.

However, these small density variations on order of the sample dimension require time to settle out of the bulk as observed in Lei *et al.* [30] As a collective whole, these fluctuations induce large-scale velocity fluctuations (convection) and are carried out of suspension in advance of the suspension solvent interface. On the other hand, the moving interface has an advantage that it is not perturbed from above by such fluctuations and a density gradient, which is the definition of an interface, quenches rising low-density fluctuations [33,43] and stabilizes the interface. So there are reasons to expect the more rapid organization at the interface compared to the bulk. It is the absence of these fluctuations that leads to a slower interface sedimentation velocity and absence of velocity fluctuations.

## V. CONCLUSION

We have carried out an experimental study of sedimentation of monodisperse polystyrene latex spheres in an aqueous solution. Salt is added to the solution so that the charged polystyrene particles are highly screened and behave effectively as hard spheres. The mean sedimentation velocity is measured as a function of the particle volume fraction for suspensions with different Péclet numbers. New sedimentation measurements are made for selected suspensions undergoing a simple shear flow, which is applied to destroy local and global interparticle structures. The measurements support the contention that the high-Pe systems are more ordered than the low-Pe systems. The measured concentration dependence of the mean sedimentation velocity, as a function of Péclet number, shows that low-Pe systems produce Batchelor results with the particle configurations being continually randomized by Brownian motion. On the other hand, high-Pe

systems demonstrate the “nonanalytic” form given in Eq. (3), which is also produced in low-Pe suspensions, but with strong long-ranged charge interactions. Here Brownian motion is not sufficient to randomize the inter-particle order. Evidently the concentration fluctuations above and below the average exit the system during the sedimentation, leaving the suspension more uniform. The sedimentation measurements in suspensions undergoing shear while settling support this view. Increasing rate of shear disrupts this ordering in the

suspension and produces more rapid settling. The ordering occurs more rapidly at the upper interface than in the bulk due, possibly, to other processes active in the interface and the development of a concentration gradient.

#### ACKNOWLEDGMENTS

P. T. was supported in part by the Research Grants Council of Hong Kong SAR under Grant No. HKUST603305.

- 
- [1] T. W. Oppel, W. K. Myers, and C. S. Keefer, *J. Clin. Invest.* **12**, 291 (1933).
- [2] P. Y. Cheng and H. K. Schachman, *J. Polym. Sci.* **16**, 19 (1955).
- [3] G. K. Batchelor, *J. Fluid Mech.* **52**, 245 (1972).
- [4] P. Mazur and W. van Saarloos, *Physica A* **115**, 21 (1982).
- [5] S. E. Paulin and B. J. Ackerson, *Phys. Rev. Lett.* **64**, 2663 (1990).
- [6] K. E. Davis, W. B. Russel, and W. J. Glantschnig, *J. Chem. Soc., Faraday Trans.* **87**, 411 (1991).
- [7] D. M. E. Thies-Weesie, A. P. Philipse, G. Nagele, B. Mandl, and R. Klein, *J. Colloid Interface Sci.* **176**, 43 (1995).
- [8] H. C. Brinkman, *Appl. Sci. Res., Sect. A* **1**, 27 (1947).
- [9] S. Childress, *J. Chem. Phys.* **56**, 2527 (1972).
- [10] P. G. Saffman, *Stud. Appl. Math.* **52**, 115 (1973).
- [11] E. J. Hinch, *J. Fluid Mech.* **83**, 695 (1977).
- [12] H. Hasimoto, *J. Fluid Mech.* **5**, 317 (1959).
- [13] A. A. Zick and G. M. Homsy, *J. Fluid Mech.* **115**, 13 (1982).
- [14] A. S. Sangani and G. Mo, *Phys. Fluids* **8**, 1990 (1996).
- [15] D. R. Oliver, *Chem. Eng. Sci.* **15**, 230 (1961).
- [16] E. M. Tory, M. Barfiel, and M. T. Kamel, *Powder Technol.* **74**, 159 (1993).
- [17] B. Koglin, in *Particle Size Analysis 1970*, edited by M. J. Groves and J. L. Wyatt-Sargent (Society of Analytical Chemistry, London, 1972), p. 223; *Chem.-Ing.-Tech.* **44**, 515 (1972).
- [18] J. Happel and H. Brenner, *Low Reynolds Number Hydrodynamics* (Nijhoff, Dordrecht, 1983).
- [19] R. H. Davis and M. A. Hassen, *J. Fluid Mech.* **196**, 107 (1988).
- [20] R. Johne, D. L. Koch, and E. S. G. Shaqfeh, *J. Fluid Mech.* **224**, 275 (1991).
- [21] R. P. Boardman, M.Sc. thesis, London University, 1961.
- [22] B. Koglin, *DECHEMA-Monogr.* **79B**, 1589 (1976).
- [23] E. M. Tory and D. K. Pickard, *Chem. Eng. Sci.* **55**, 655 (1977).
- [24] B. Koglin, Ph.D. dissertation, Universitat Karlsruhe, 1971.
- [25] R. E. Calfish and J. H. Luke, *Phys. Fluids* **28**, 759 (1985).
- [26] H. Nicolai and E. Guazzelli, *Phys. Fluids* **7**, 3 (1995).
- [27] P. N. Segre, E. Herbolzheimer, and P. M. Chaikin, *Phys. Rev. Lett.* **79**, 2574 (1997).
- [28] M. L. Cowan, J. H. Page, and D. A. Weitz, *Phys. Rev. Lett.* **85**, 453 (2000).
- [29] E. Guazzelli, *Phys. Fluids* **13**, 1537 (2001).
- [30] X. Lei, B. J. Ackerson, and P. Tong, *Phys. Rev. Lett.* **86**, 3300 (2001).
- [31] S.-Y. Tee, P. J. Mucha, L. Cipelletti, S. Manley, M. P. Brenner, P. N. Segre, and D. A. Weitz, *Phys. Rev. Lett.* **89**, 054501 (2002).
- [32] L. Bergougnoux, S. Ghicini, E. Guazzelli, and J. Hinch, *Phys. Fluids* **15**, 1875 (2003).
- [33] J. H. C. Luke, *Phys. Fluids* **12**, 1619 (2000).
- [34] P. J. Mucha and M. P. Brenner, *Phys. Fluids* **15**, 1305 (2003).
- [35] B. U. Felderhof, *Physica A* **348**, 16 (2005).
- [36] A. J. C. Ladd, *Phys. Fluids A* **5**, 299 (1993).
- [37] A. J. C. Ladd, *Phys. Rev. Lett.* **76**, 1392 (1996).
- [38] A. J. C. Ladd, *Phys. Fluids* **9**, 491 (1997).
- [39] A. J. C. Ladd, *Phys. Rev. Lett.* **88**, 048301 (2002).
- [40] N.-Q. Nguyen and A. J. C. Ladd, *Phys. Rev. E* **69**, 050401(R) (2004).
- [41] G. Bernard-Michel, A. Monavon, D. Lhuillier, D. Abdo, and H. Simon, *Phys. Fluids* **14**, 2339 (2002).
- [42] N.-Q. Nguyen and A. J. C. Ladd, *J. Fluid Mech.* **525**, 73 (2005).
- [43] P. J. Mucha, S.-Y. Tee, D. A. Weitz, B. I. Shraiman, and M. P. Brenner, *J. Fluid Mech.* **501**, 71 (2004).
- [44] D. Bruneau, R. Anthore, F. Feuillebois, X. Auvray, and C. Petipas, *J. Fluid Mech.* **221**, 577 (1990).
- [45] D. M. Mueth, J. C. Crocker, S. E. Esipov, and D. G. Grier, *Phys. Rev. Lett.* **77**, 578 (1996).
- [46] B. J. Ackerson and N. A. Clark, *J. Phys. (Paris)* **42**, 929 (1981).
- [47] G. I. Taylor, *Philos. Trans. R. Soc. London, Ser. A* **223**, 289 (1923).
- [48] R. H. Davis and K. H. Birdsell, *AIChE J.* **34**, 123 (1988).
- [49] *Handbook of Chemistry and Physics*, edited by C. D. Hodgman (Chemical Rubber, Cleveland, 1951).
- [50] B. J. Ackerson, S. E. Paulin, B. Johnson, W. Van Megen, and S. A. Underwood, *Phys. Rev. E* **59**, 6903 (1999).
- [51] W. B. Russel, D. A. Savile, and W. R. Schowalter, *Colloidal Dispersions* (Cambridge University Press, Cambridge, UK, 1989).
- [52] T. J. Hanratty and A. Bandukwala, *AIChE J.* **3**, 293 (1957).
- [53] J. M. Ham and G. M. Homsy, *Int. J. Multiphase Flow* **14**, 533 (1988).
- [54] M. Watzlawek and G. Nagele, *J. Colloid Interface Sci.* **214**, 170 (1999).
- [55] E. J. Hinch, in *Disorder and Mixing*, edited by E. Guyon, J.-P. Nadal, and Y. Pomeau (Kluwer Academic, Dordrecht, 1988).
- [56] A. Levine, S. Ramaswamy, E. Frey, and R. Bruinsma, *Phys. Rev. Lett.* **81**, 5944 (1998).